JOURNAL OF GEOPHYSICAL RESEARCH, VOL. 114, A00C18, doi:10.1029/2008JA013498, 2009

Observation and modeling of the injection observed by THEMIS and LANL satellites during the 23 March 2007 substorm event

W. L. Liu,[1,2] X. Li,[1,2] T. Sarris,[1] C. Cully,[3] R. Ergun,[1] V. Angelopoulos,[4] D. Larson,[5] A. Keiling,[5] K. H. Glassmeier,[6] and H. U. Auster[6]

Received 14 June 2008; revised 20 October 2008; accepted 1 December 2008; published 24 February 2009.

[1] During the encounter of a substorm on 23 March 2007, the THEMIS constellation observed energetic particle injections and dipolarizations in the premidnight sector. Clear injection and dipolarization signatures were observed during the main intensification by three probes (A, B, and D) in the region around 11 R_E and 2100 local time (LT). THEMIS C, which was leading in the constellation at 8.3 R_E, also observed a clear injection signature, but the dipolarization was not so clear. From the timing based on these observations, a fast westward expanding ion injection and dipolarization front was identified. In combination with the energetic particle observations from Los Alamos National Laboratory (LANL) geosynchronous satellites, the particle injection seemed to initiate between 2100 and 0100 LT. This event provides an excellent opportunity to examine the dipolarization and particle injection processes beyond geosynchronous orbit and over a wide LT range. We model this injection event by means of test particle simulation, setting up an initial particle distribution and sending an earthward dipolarization-like pulse from the tail that also expands azimuthally, then recording the ions and electrons at the various satellite locations. Most features of the injected particles are reproduced by the test particle simulation. These include not only the earthward injections but also the fast westward expansion of the injection, as well as the timing of the injections as observed among different satellites that made the observations. On the basis of the observations and the simulation results, we suggest that this substorm injection was initiated around 2300 LT, farther down the tail, and propagated radially inward and expanded azimuthally.

Citation: Liu, W. L., X. Li, T. Sarris, C. Cully, R. Ergun, V. Angelopoulos, D. Larson, A. Keiling, K. H. Glassmeier, and H. U. Auster (2009), Observation and modeling of the injection observed by THEMIS and LANL satellites during the 23 March 2007 substorm event, *J. Geophys. Res.*, *114*, A00C18, doi:10.1029/2008JA013498.

1. Introduction

[2] Injections of energetic particles of tens to hundreds of keV at geosynchronous orbit are among the main features during substorms [e.g., *McIlwain*, 1974; *Kivelson et al.*, 1980]. The injections can be observed with or without energy dispersion, depending on the relative location of the measurements with respect to the initial injection. Dispersionless injections indicate that fluxes of particles with different energies increase at the same time, which are usually observed in the ''injection region'' near local midnight. When injected particles of different energies drift out of the injection region, energy dispersion is expected because of their different drift velocities [*McIlwain*, 1974; *Mauk and Meng*, 1987; *Reeves et al.*, 1996].

[3] In order to explain the injections observed at geosynchronous orbit, the ''injection boundary'' model was proposed by *McIlwain* [1974]. In this model, it was suggested that a spatial boundary formed during the injection to separate the newly injected particles from the preexisting particles. It was assumed that, behind this boundary, particles were energized together and should be observed without dispersion. The mechanism of this simultaneous energization was not addressed by the injection boundary. This model has been further explored [e.g., *Mauk and McIlwain*, 1974; *Konradi et al.*, 1975; *Mauk and Meng*, 1987]. However, on the basis of test particle simulation results [*Li et al.*, 1998], it was suggested that the injection boundary is not necessary for explaining the dispersionless injection. In the model by *Li et al.* [1998], dispersionless injections are well reproduced by an earthward propagating

[1]LASP, University of Colorado, Boulder, Colorado, USA.
[2]Laboratory for Space Weather, Chinese Academy of Sciences, Beijing, China.
[3]Swedish Institute of Space Physics, Uppsala, Sweden.
[4]IGPP, University of California, Los Angeles, California, USA.
[5]SSL, University of California, Berkeley, California, USA.
[6]IGEP, Technical University of Braunschweig, Braunschweig, Germany.

0148-0227/09/2008JA013498$09.00

electric field pulse. This model was further developed by *Sarris et al.* [2002] and *Sarris and Li* [2005].

[4] The THEMIS mission, consisting of five small satellites and a ground-based observatory network [*Angelopoulos*, 2008], is designed to answer longstanding questions concerning the nature of the substorm. On 23 March 2007, two substorm events were observed by THEMIS in situ during its cost phase and ground-based measurements: one at 1110 UT, and one at 1119 UT. The event around 1110 UT has already been investigated by several researchers [*Angelopoulos et al.*, 2008; *Raeder et al.*, 2008; *Keiling et al.*, 2008a, 2008b]. Multiple activities in the plasma sheet are reported by *Keiling et al.* [2008b], who demonstrated that several enhancements of energetic particle fluxes observed by THEMIS satellites could be one-to-one correlated with the intensifications in auroral structures. However, Los Alamos National Laboratory (LANL) satellites at geosynchronous orbit observed clearly only one injection of energetic electrons and protons, which was associated with the most intense auroral intensification around 1119 UT. In this paper, we will focus on this main intensification and discuss the energetic particle injection and its propagation. Data from THEMIS satellites and LANL satellites are analyzed to characterize this event. A test particle simulation is carried out to model this event. Consistency is reached between observations and simulation results.

2. Orbit and Instruments

[5] The five THEMIS satellites were successfully launched on 17 February 2007. During its coast phase from March to September 2007, the five satellites were placed in the same orbit with an apogee of 14.7 R_E and a perigee of 1.07 R_E. The locations of the THEMIS constellation and LANL satellites at 1120 UT on 23 March are shown in Figure 1. The detailed positions of THEMIS satellites in the GSM coordinate system are tabulated in Table 1. At that time, THEMIS satellites were in their inbound orbits. THEMIS C was leading while THEMIS E was trailing. The other three probes D, B and A were closely spaced in between probes C and E. There were two LANL satellites near the nightside at geosynchronous orbit at that time, LANL-97A at ~2100 LT and 1989−046 at ~0100 LT.

3. Observations

[6] The observations presented in this paper are from the fluxgate magnetometers (FGM) [*Auster et al.*, 2008] and solid state telescopes (SST) [*Larson et al.*, 2009] onboard five THEMIS satellites and SOPA instruments onboard LANL geosynchronous satellites [*Belian et al.*, 1992].

[7] The substorm event occurred during the main phase of a moderate storm with a minimum *Dst* index of −80 nT. From ACE solar wind data, an IMF northward turning was identified at 0925 UT with a dynamic pressure enhancement. This northward turning was later observed by the Cluster constellation right outside the magnetosheath at 1108 UT.

[8] An overview of THEMIS FGM and SST observations is shown in Figure 2. From the magnetic field data of D, B, and A, clear dipolarizations can be identified with the increase of B_z magnitude and the decrease of B_x magnitude, at the times marked by the solid lines. The time sequence of dipolarizations is D → B → A, indicating an azimuthal expansion from east to west. On the basis of the time difference, the westward propagation speed of the dipolarization signal can be estimated at 150~200 km/s, or 5~8 deg/min.

[9] From SST energetic ion data (63~278 keV) shown in Figure 2, nearly dispersionless injections can also be seen as marked by the dashed lines. The time sequence of the injections is the same as that of the observed dipolarizations. *Angelopoulos et al.* [2008] analyzed the motion of the energized plasma and considered the finite gyroradius effect. They identified lobeward expansions during the injections and interpreted that the time delays are partly due to the lobeward expansion of the hot plasma sheet. However, the expansions are clearly associated with the dipolarizations/injections and we will argue here that the time delays are due to the propagation of the dipolarizations/injections.

[10] Although THEMIS C also observed the injection, the injection was only obvious in high-energy channels (>100 keV). THEMIS C did not observe a clear dipolarization in the magnetic field data, which may be due to its location: THEMIS C was 0.05 R_E lower than THEMIS D in the GSM coordinate system and about 3 R_E closer to the Earth, so it is possible that THEMIS C was below the lower edge of the plasma sheet and did not measure the magnetic field variations in the plasma sheet. The observation of flux enhancements only in high-energy channels at THEMIS C can be explained by the fact that high-energy ions with large gyroradius can reach THEMIS C, whereas low-energy ions with small gyroradius cannot [*Angelopoulos et al.*, 2008]. THEMIS E, which was farther west of D, observed intense fluctuations in the magnetic field but did not observe the dipolarization as THEMIS D, B, A did.

[11] Energetic particle data from all available LANL satellites are shown in Figure 3. From top to bottom, the data are shown in the eastward LT sequence from midnight (refer to Figure 1). Midnight was between LANL-97A and 1989−046, and it can be seen from Figure 3 that these two satellites observed quite different phenomena: The premidnight satellite, LANL-97A, observed an ion injection with some energy dispersion at 1120 UT but no electron injection, whereas the postmidnight satellite, 1989−046, observed a dispersionless electron injection at 1122 UT but no ion injection. The drift motions of the injected particles (westward for ions and eastward for electrons) can be identified from the delay in the appearance of the injection among these spacecrafts. Drift echoes can also be identified, primarily in lower-energy channels. On the basis of the observations, we can conclude that the center of injection was between LANL-97A and 1989−046. However, the radial location of the injection initiation cannot be determined solely on the basis of geosynchronous observations.

[12] Figure 4 shows the timing of ion injections measured by THEMIS C, D, LANL-97A and electron injection measured by 1989−046. The injection was first observed by THEMIS C at 1118 UT. THEMIS D observed it one minute later at ~1119 UT. Then LANL-97A and 1989−046 measured ion and electron injection at ~1120 UT and ~1122 UT, respectively. The timing suggests an earthward propagating and azimuthally expanding injection front.

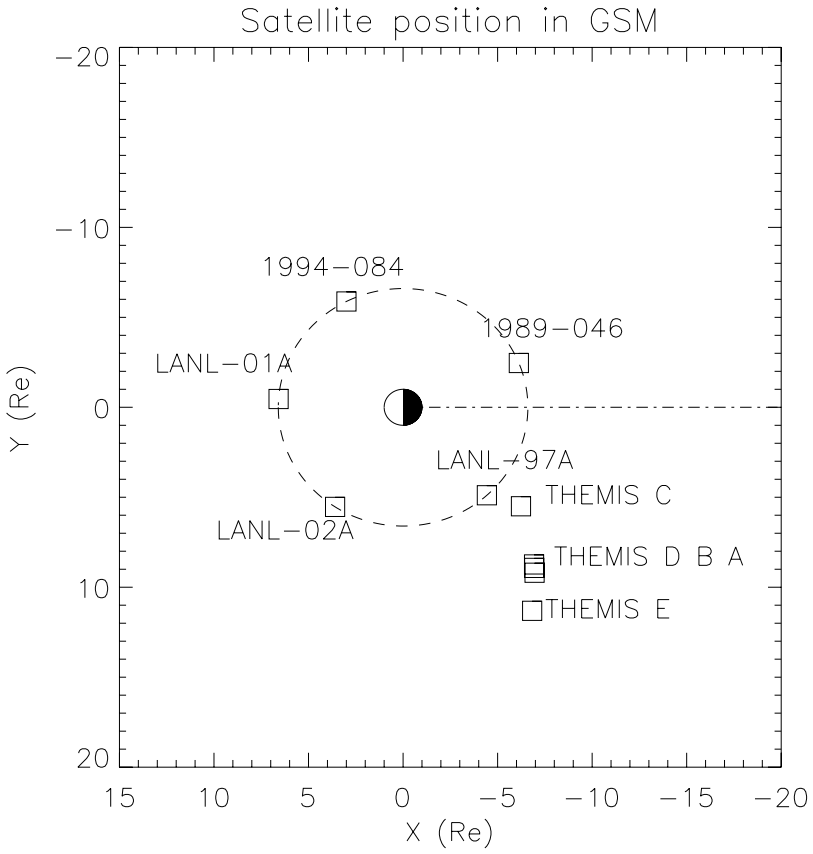

Figure 1. THEMIS and LANL satellite positions in GSM coordinate system at 1120 UT on 23 March 2007.

[13] This is an excellent event which provides us the opportunity to observe dipolarization/injections at multiple points at and beyond geosynchronous orbit. However, questions that still remain are the following: (1) were the initial enhancements of protons and electrons measured by THEMIS and LANL as shown in Figures 3 and 4 from one single injection? and (2) where were the injections initiated (their source populations)? We will conduct test particle simulations to address these questions.

4. Test Particle Simulation

[14] The model in this paper is evolved from *Li et al.* [1998] and *Sarris et al.* [2002] models; the new feature of a fast azimuthal expansion velocity was not included in the previous models. An earthward dipolarization of the magnetic field will result in an inductive electric field and the perturbation starts first at near midnight and spreads in azimuth in both directions. The dawn-dusk component of the electric field, which also propagates earthward, can cause the charged particles to move earthward, following the motion of the $\mathbf{E} \times \mathbf{B}$ drift. In this process, the particles will be energized through betatron acceleration. In this paper, the electric field E_ϕ is given in a spherical coordinate system (r, θ, ϕ) by the following expression:

$$\mathbf{E}_\phi = -\hat{e}E_0(1 + c_1\cos(\phi - \phi_0))^p \exp(-\xi^2), \qquad (1)$$

where $r = 0$ at the center of the Earth, $\theta = 0$ at the equatorial plane and $\phi = 0$ at local noon, $\xi = [r - r_i + v(r)(t - t_\alpha)]/d$ determines the location of the maximum value of the pulse; $v(r) = a + br$ is the pulse front velocity as a function of radial distance r; d is the radial width of the pulse; c_1 (>0) and p (>0) describe the LT dependence of the electric field amplitude, which is largest at ϕ_0, the LT of the injection center; $t_\alpha = (c_2 R_E/v_\alpha)(1 - cos(\phi - \phi_0))$ represents the delay of the pulse from ϕ_0 to other LTs; c_2 determines the magnitude of the delay; v_α is the longitudinal propagation speed of the pulse; and r_i is a parameter in the simulation that determines the arrival time of the pulse. In this paper we present results with $\phi_0 = 165°$, $E_0 = 1.3 \times 10^{-4} mV/m$, $c_1 = 1$, $c_2 = 0.5\ R_E$, $a = 100\ km/s$, $b = 0.0145\ s^{-1}$, $p = 14$, $v_\alpha = 150\ km/s$,$r_i = 90\ R_E$, and $d = 3.0 \times 10^4\ km$. The magnetic field of the pulse is obtained from Faraday's law [*Sarris et al.*, 2002]. These parameters create the pulse with the best agreement with the observed B_z signatures, as discussed below.

[15] Using the above parameters in equation (1) translates to an earthward propagating pulse generated at 2300 LT.

Table 1. Satellite Locations in GSM Coordinate System at 1120 UT

R_E	A	B	C	D	E
X	−6.96	−6.94	−6.23	−6.93	−6.83
Y	9.4	9.22	5.93	9.04	11.51
Z	−0.57	−0.58	−0.64	−0.59	−0.46

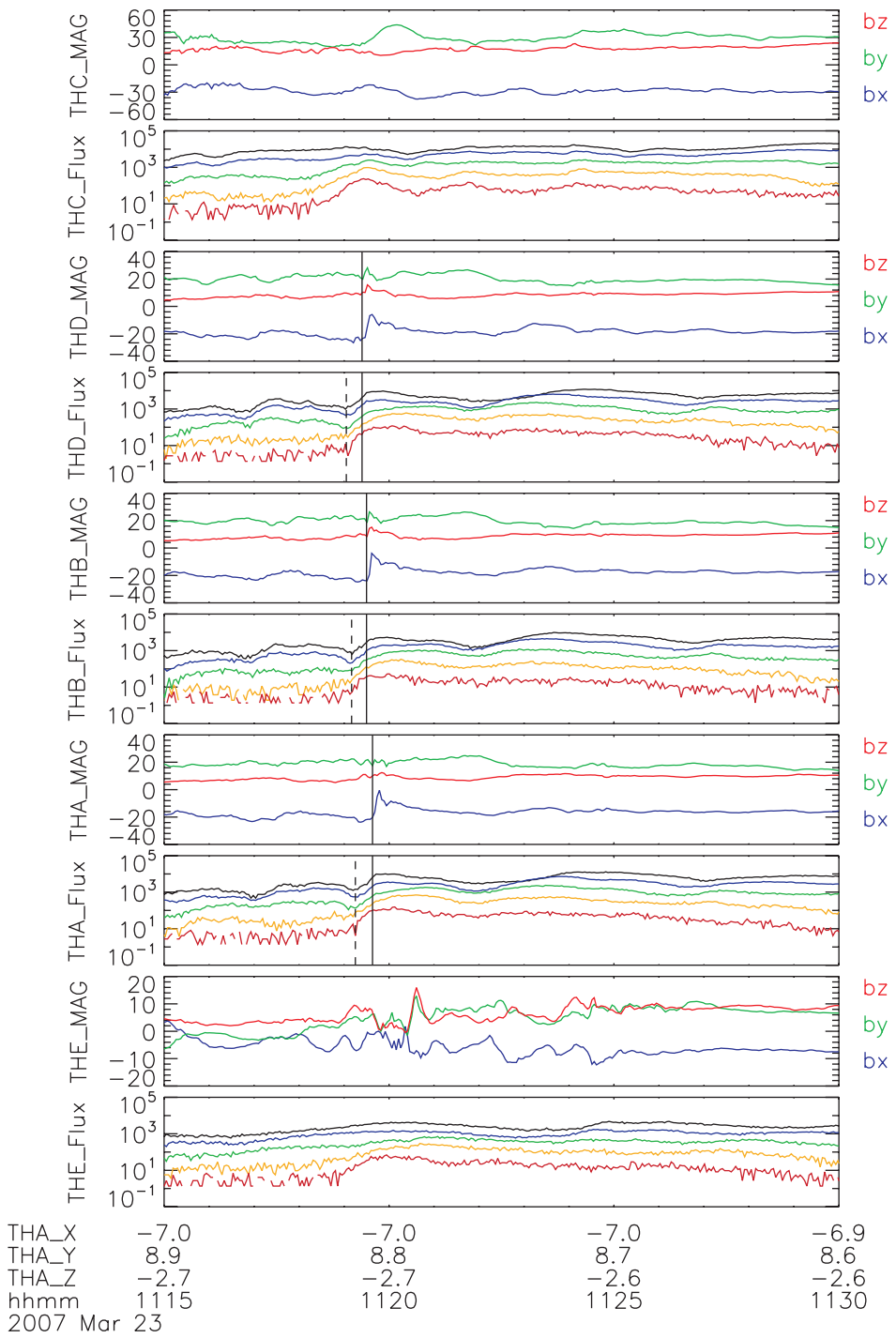

Figure 2. THEMIS magnetic field (nT in GSM) and energetic proton flux (63∼278 keV, number per $cm^2\ s^{-1}\ sr^{-1}\ keV^{-1}$) observations during the 23 March event showing data of (top to bottom) THEMIS C, D, B, A, and E. Solid and dashed vertical lines mark the beginners of dipolarizations and injections, respectively.

The radial pulse electric field and pulse magnetic field plus a background dipole field at the center of the pulse (2300 LT) at t = 400 s are illustrated in Figure 5a. The comparison between modeled and observed B_z component at THEMIS satellite locations are shown in Figure 5b. It should be noted that the total field in our model is the pulse field plus a background dipole field and there is no plasma sheet in our model. Thus the B_x and B_y components are not considered and the background B_z value in the simulation is greater than that in the observation. The vertical scales of each satellite in Figure 5b are the same, but the base value of modeled B_z is greater than the observed base value. The B_z increases in this model at THEMIS D, B, A's locations compare reasonably well with the observations as shown in

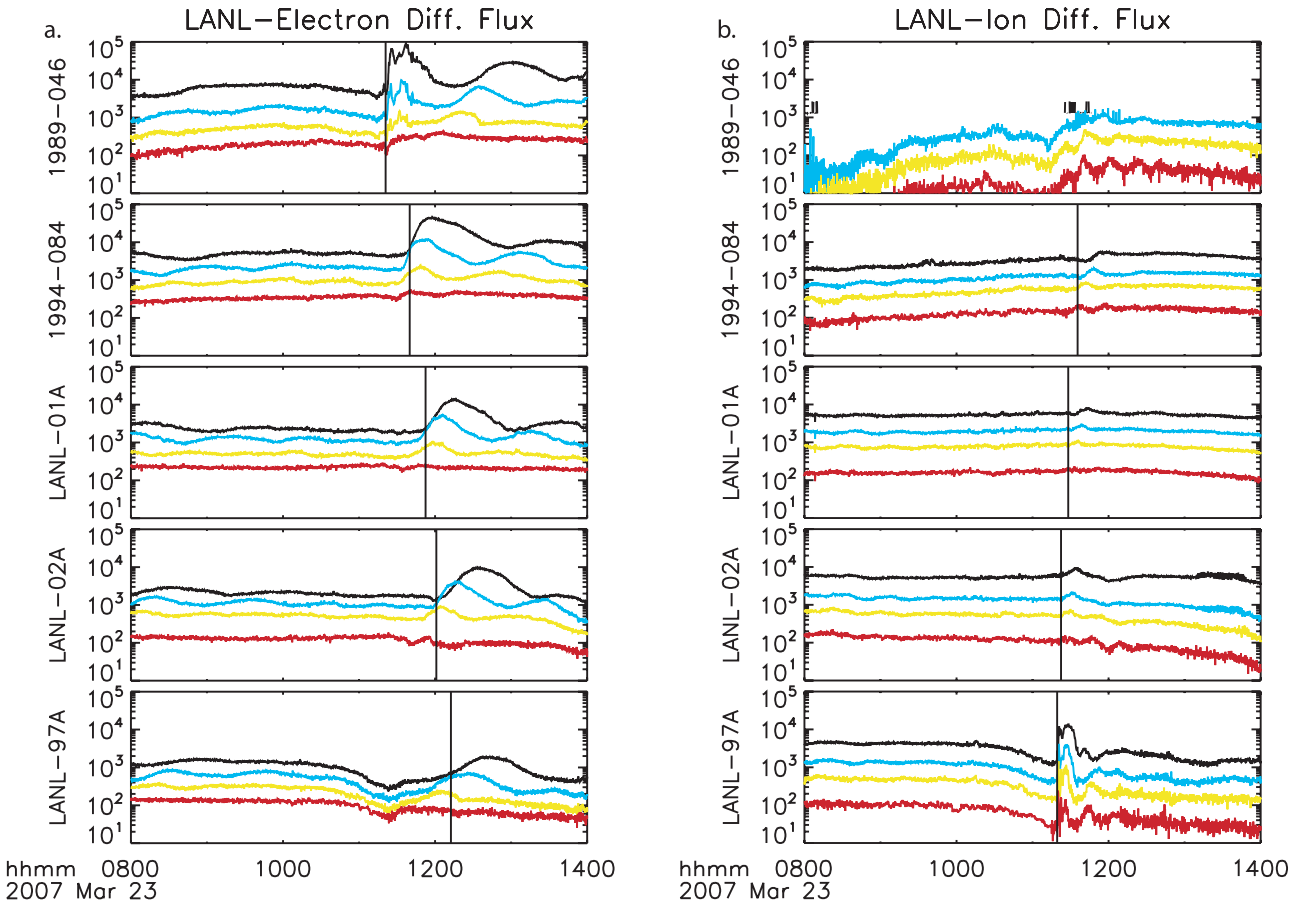

Figure 3. LANL energetic (a) electron and (b) proton observations. Shown are (top to bottom) 1989–046, 1994–084, LANL-01A, LANL-02A, and LANL-97A data. The energy range is 75∼500 keV for electrons and 75∼400 keV for protons. Vertical lines mark the injection times at different satellite positions.

Figure 5b. However, as discussed above in section 3, THEMIS C was below the plasma sheet and didn't observed the dipolarization. THEMIS E was farther away from the Earth and from the injection center. Our model field there shows a smaller B_z increase, but the timing is still reasonable. The comparison at geosynchronous orbit are not included because the GOES spacecraft were far away from the injection center and LANL spacecraft don't have magnetic measurements, though the direction of the magnetic field can be derived from the symmetries of the measured plasma distribution. However, the modeled B_z variation at geosynchronous orbit (from the same model field but with different parameters) had been compared with GOES measurements for other events, they were in good agreement [e.g., *Li et al.*, 2003]. We are confident that the magnetic field direction at LANL spacecrafts, 1989–046 and LANL-97A, should become dipolarized when they observed the dispersionless injections of particles, on the basis of previous studies [*Birn et al.*, 1997a, 1997b, 1998; *Li et al.*, 1998, 2003]. The booms of the electric field instrument (EFI) onboard THEMIS were not deployed at that time, so there is no comparison between the modeled and measured electric field.

[16] We traced 500,000 protons and 500,000 electrons initially distributed randomly in the radial distance between 6 R_E and 25 R_E and at all LTs in the equatorial plane with 90° pitch angles. The initial energies are from 6 keV to 418 keV with an increment step of 5%. Particles that reach as close as 1.0 R_E to the THEMIS and LANL satellite locations are recorded.

[17] Particle weighting was given as the formation described by *Li et al.* [1998]. The initial radial dependence was given by *Li et al.* [1998, equation (2)] with

$$f_r = \left[\frac{(r_0 - a_0)^{nl}}{r_0^{ml}}\right] \Big/ \left[\frac{(a_0 d - a_0)^{nl}}{a_{0d}^{ml}}\right], \qquad (2)$$

where $a_0 = 3$, $nl = 4$, $ml = 10$, $a_{0d} = 6$ for electron and $a_0 = 4$, $nl = 6$, $ml = 10$, $a_{0d} = 6$ for proton. The initial energy dependence is given by the kappa distribution with kappa = 2.1 in the region $r < 12$ R_E estimated on the basis of the measurements from THEMIS and LANL satellites during the quiet time before this substorm onset, and kappa = 5.3 in the region $r \geq 12$ R_E, which is the average kappa value calculated in the previous statistical study on the basis of ISEE 1 data beyond 12 R_E [*Christon et al.*, 1989, 1991].

[18] By applying the weighting functions described by *Li et al.* [1998], particles are assumed to be representative of ensembles of particles. We subsequently construct particle

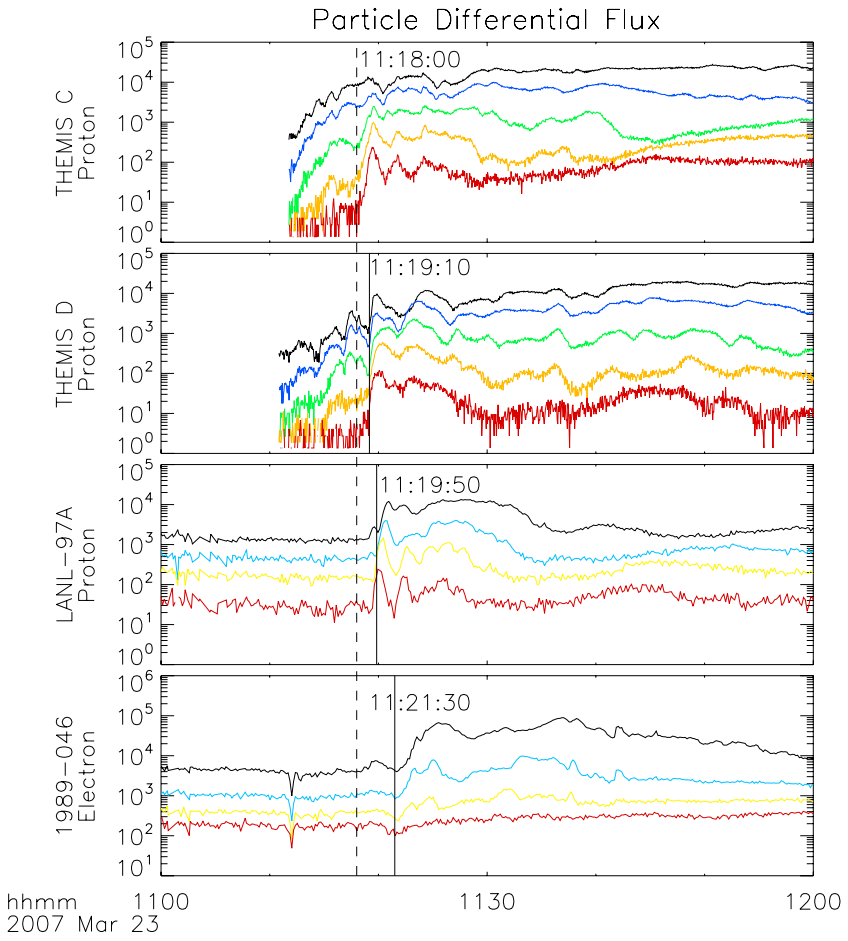

Figure 4. Injection timing between satellites THEMIS C and D, LANL-97A, and 1989−046 during the 23 March event. The dashed vertical line marks the first injection signature observed by THEMIS C. Solid vertical lines mark the injection signature observed by THEMIS D, LANL97A, and 1989−046.

fluxes by summing the weighted particles that are recorded at THEMIS and LANL locations in the simulation. The results are shown in Figure 6. We can see that the basic features of this event are reproduced. In the simulation, the proton injections only appear at THEMIS C, D and LANL-97A locations, which are west of the center of the pulse, whereas the electron injection is only measured by 1989−046, which is located east of the center of the pulse. The magnitude of flux enhancement is consistent with the observations. Furthermore, the timing of flux increases between these satellites in this simulation is about the same as the observations. Thus we can now answer question 1 raised in section 3 that the initial enhancement of the particles measured by various satellites widely spread in radial distance and local times, as shown in Figures 2, 3, and 4, is from one single injection. We will address question 2 in section 5.

5. Discussion

5.1. Fast Westward Expansion

[19] Before we address the initiation location of the injection, we would like to discuss the fast westward expansion of the dipolarization, which is a longstanding topic in substorm research. Several studies investigated the expansion speed at geosynchronous orbit [e.g., *Kokubun and McPherron*, 1981; *Nagai*, 1982; *Lopez et al.*, 1990; *Liou et al.*, 2002]. On the basis of a statistical study of GOES observations by *Liou et al.* [2002], the westward expansion speed was estimated to be 4.9 deg/min (60 km/s at 6.6 R_E). On the basis of the observations presented here, the expansion speed is estimated to be 5∼8 deg/min, which is comparable to the values in previous works at geosynchronous orbit, but the linear speed at THEMIS location is faster, 150∼200 km/s. This feature is captured in our model. The observations of westward expansion are consistent with the hypothetical earthward propagating and expanding electric field pulse in this paper.

5.2. Transport of Energetic Particles

[20] In Figure 5a we plot the radial profile of the model magnetic field. As Figure 5a shows, the pulse field creates a "well" in this profile as it moves toward the Earth. This well can affect the gradient B drift of particles. For example, in the bottom of this well located at ∼12 R_E in this snapshot, where gradient B is close to 0, the particles will stop their azimuthal gradient B drift and will be transported toward the Earth because of the $\mathbf{E} \times \mathbf{B}$ drift. These particles will be energized by betatron acceleration and injected into the near Earth region. However, if a particle meets the pulse at or

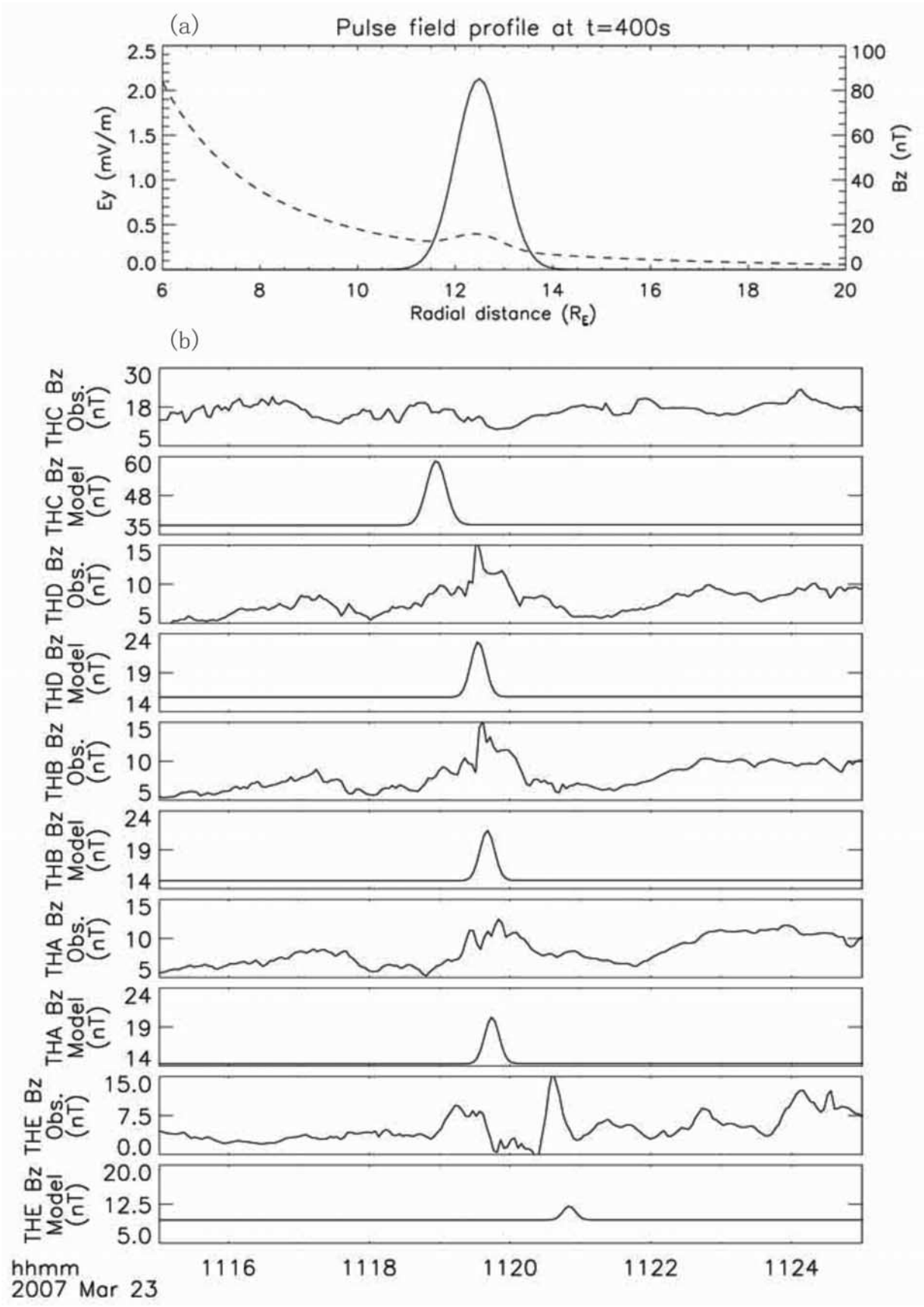
(a)
Pulse field profile at t=400s
Ey (mV/m)
Bz (nT)
Radial distance (R_E)
(b)
THC Bz Obs. (nT)
THC Bz Model (nT)
THD Bz Obs. (nT)
THD Bz Model (nT)
THB Bz Obs. (nT)
THB Bz Model (nT)
THA Bz Obs. (nT)
THA Bz Model (nT)
THE Bz Obs. (nT)
THE Bz Model (nT)
hhmm
2007 Mar 23

Figure 5

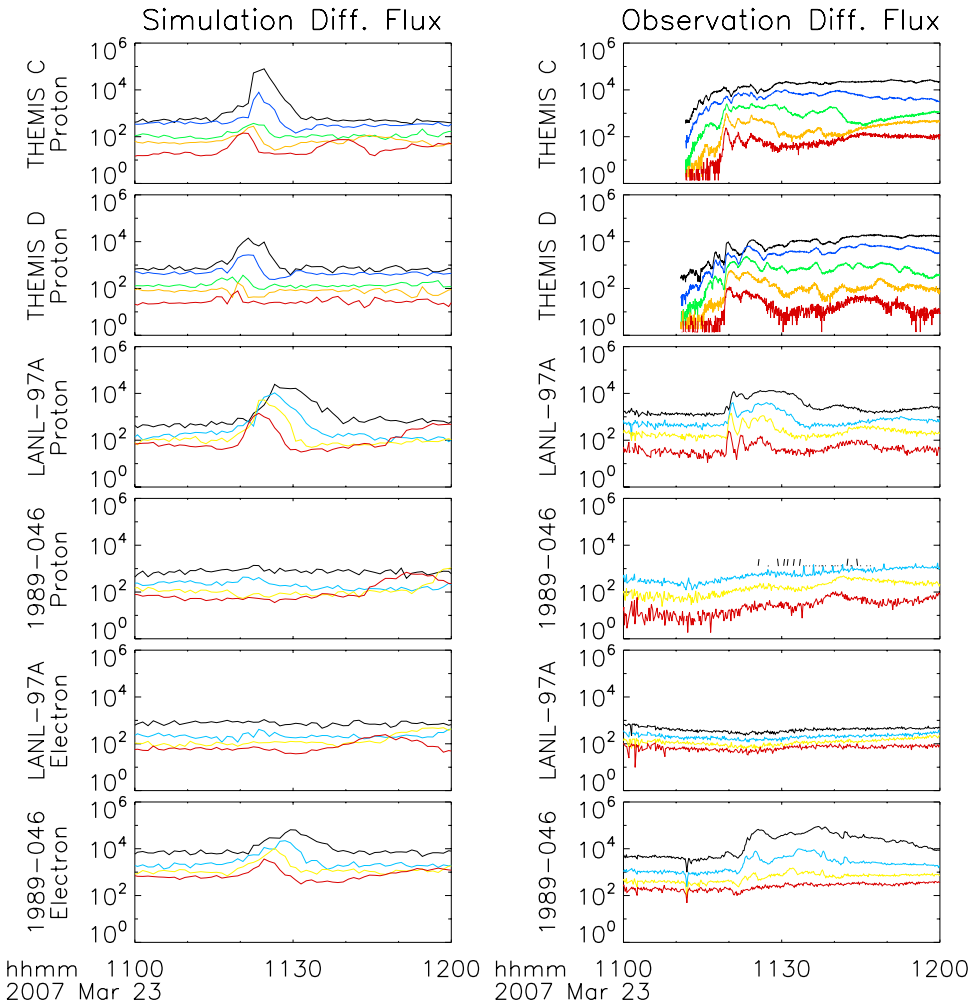

Figure 6. Comparison between (left) simulation and (right) observation of particle differential fluxes. The first four panels represent proton fluxes at THEMIS C, THEMIS D, LANL-97A, and 1989–046, respectively. The last two panels represent electron fluxes at LANL-97A and 1989–046, respectively.

after the pulse peak, its drift motion will not be affected as much and it will not be effectively transported by the pulse. Thus the temporal profile of the pulse field should be consistent with the temporal profile of particle flux. This is demonstrated in the modeled flux of THEMIS D, B and A, as shown in Figure 6, and is consistent with the fluxes observations at THEMIS D, B and A, as shown in Figure 2.

5.3. Location of Initial Diploarization

[21] When we trace the particles in our simulation, we find that the maximum initial radial distance of the particles "measured" at THEMIS D's location is 20 R_E. This means the model field used in this paper can bring inward particles which are as far as 20 R_E. The model field has to initiate beyond 20 R_E to sweep the particles inward and produce the injections, which are comparable to the observations. Although the exact value of the maximum initial distance may vary on the basis of the parameters chosen in the model, we suggest that the initiation of the dipolarization has to be farther down the tail for this event.

[22] In order to identify the source locations of the injected particles, we set different threshold values to the initial radial distance r_0 (see equation (2)), as shown in Figure 7. From top to bottom, the plots in Figure 7 represent the simulated ion differential fluxes at the THEMIS D position with the thresholds $r_0 < 15$, 17,21 R_E, respectively. Figure 7 shows that if there were a lack of source particles at larger radial distances, a virtual satellite at THEMIS D's position would not measure the injection as THEMIS D did. We see that the injected particles measured by THEMIS D mainly come from the region beyond 17 R_E.

[23] The comparison between observations and the simulation results suggests that this simple model can reproduce most of the features in this event. On the basis of the

Figure 5. (a) The profiles of pulse electric field E_y (solid line) and pulse magnetic field B_z plus a background dipole field (dashed line) at 2300 LT at $t = 400$ s. (b) Comparison between observed and modeled B_z component at THEMIS locations. The magnetic field in the model is plotted as the pulse field pulse a background dipole field. The vertical scales of each satellite are the same, but the base value of the model field is greater than the observed base value.

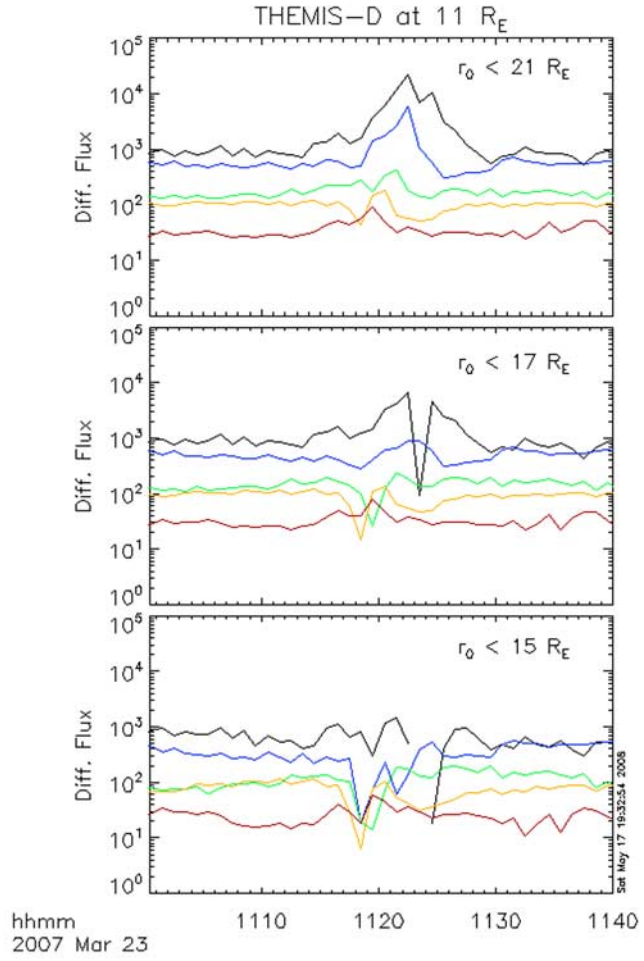

Figure 7. Simulated ion differential fluxes (63∼278 keV) at THEMIS D's location with particle initial radial distance thresholds (top to bottom) r_0 < 21, 17, and 15 R_E.

observation only, we can tell that the injection occurred between two LANL satellites: LANL-97A and 1989−046, see Figure 1 for reference. On the basis of several runs of the simulations, we found that the center of the model field for this event was best set at 2300 LT, which is considered to be the center of the injection front of this event. On the basis of the OpenGGCM simulation with the input of solar wind observation, *Raeder et al.* [2008] suggested that the initial location of this dipolarization was around $X_{GSE} = -20R_E$ and duskward of the tail center, which is consistent with our conclusion.

[24] In the outside-in substorm scenario, the reconnection in the magnetotail generates fast flows moving toward the Earth. These fast flows brake in the near Earth region and are responsible for the substorm onset. The earthward propagation of the pulse field represents these fast flows from the viewpoint of our model. The magnetic field pulse increases in the northward component in our model. The analogous effect during substorms is called a dipolarization. In the model at any given radial distance the perturbation starts first at the center of the pulse and later spreads in azimuth in both directions, This represents the expansion of the substorm current wedge [*Li et al.*, 1998]. Our simulation results imply that this substorm event is in a good agreement with the outside-in substorm scenario.

5.4. Comparison With Previous Modeling Efforts

[25] Using similar models, several papers have been published to discuss substorm injection process and compare with measurements at geosynchronous orbit [*Li et al.*, 1998, 2003; *Sarris and Li*, 2005]. *Sarris et al.* [2002] simulated an event with an earthward propagation of injection at and inside geosynchronous orbit. But there was no direct comparison of simulation results with observations beyond geosynchronous orbit. Here we simulated the injections at multiple points at and beyond geosynchronous orbit at different radial and azimuthal locations. The consistency between observations and simulation results confirms that the substorm injection not only propagates earthward, but also expands azimuthally, the latter of which has not been quantitatively addressed before.

5.5. Caveats

[26] Although the basic features in the observations are reproduced in our simulation, there are still some details that cannot be well reproduced. For example, the injection observed by THEMIS C was less energy dispersive, whereas the simulation shows some dispersion. There are perhaps two reasons. The first is that our simulation is based on a two-dimensional model and only focuses on the particles in the equatorial plane. The effects in the Z direction are not included, such as the expansion of the plasma sheet and the gyroradius effect [*Angelopoulos et al.*, 2008]. The second reason is that our simulation only models one single injection associated with dipolarization and assumes a quiet magnetospheric condition before the injection, which is an approximation. *Keiling et al.* [2008b] suggested that there were multiple particle injections during this substorm event. Here we only model the major injection, which was the only one clearly registered at geosynchronous orbit, whereas other intensifications can also affect the observations.

6. Conclusion

[27] During the substorm event on 23 March 2007, energetic particle observations from the THEMIS and LANL geosynchronous satellites show that the particle injection initiates between 2100 LT and 0100 LT: Ion injections are only observed west of this region by LANL-97A and THEMIS satellites, whereas electron injections are only observed east of this region at geosynchronous orbit by LANL satellite 1989−046. In addition, from the timing based on these observations, a fast westward expanding ion injection and dipolarization front is identified.

[28] We model this injection event by means of test particle simulation, setting up an initial particle distribution and sending an earthward dipolarization-like pulse that also expands azimuthally from the tail, then recording the ions and electrons at the various satellite locations, widely separated in local time and radial distance. Most features of the injected particles are reproduced by the simulation. The timing of the modeled injections at various satellite locations is consistent with observations, which suggests that the injection of energetic particles not only propagates earthward, but also expands azimuthally. On the basis of the

observations and the simulation results, we suggest that this substorm injection was initiated around 2300 LT and farther down the tail.

[29] **Acknowledgments.** We thank the LANL science team's effort to make the data available. We also thank the constructive comments and suggestions from both referees. This work was supported by NASA THEMIS project (NAS5-02099). Financial support for the work of the FGM Lead Investigator Team at the Technical University of Braunschweig by the German Ministerium für Wirtschaft und Technologie and the Deutsches Zentrum für Luft- und Raumfahrt under grant 50QP0402 is acknowledged. This work was also supported by NSF grant ATM-0549093 and by grants from the National Natural Science Foundation of China (40621003 and 40728005).

[30] Zuyin Pu thanks Reiner Friedel and another reviewer for their assistance in evaluating this paper.

References

Angelopoulos, V. (2008), The THEMIS mission, *Space Sci. Rev.*, *141*(1–4), 5–34, doi:10.1007/s11214-008-9336-1.

Angelopoulos, V., et al. (2008), First results from the THEMIS mission, *Space Sci. Rev.*, *141*(1–4), 5–34, doi:10.1007/s11214-008-9378-4.

Auster, H. U., et al. (2008), The THEMIS fluxgate magnetometer, *Space Sci. Rev.*, *141*(1–4), 235–264, doi:10.1007/s11214-008-9365-9.

Belian, R. D., G. R. Gisler, T. Cayton, and R. Christensen (1992), High-*Z* energetic particles at geosynchronous orbit during the great solar proton event series of October 1989, *J. Geophys. Res.*, *97*, 16,897.

Birn, J., M. F. Thomsen, J. E. Borovsky, G. D. Reeves, D. J. McComas, and R. D. Belian (1997a), Characteristic plasma properties during dispersionless substorm injections at geosynchronous orbit, *J. Geophys. Res.*, *102*, 2309.

Birn, J., M. F. Thomsen, J. E. Borovsky, G. D. Reeves, D. J. McComas, R. D. Belian, and M. Hesse (1997b), Substorm ion injections: Geosynchronous observations and test particle orbits in three-dimensional dynamic MHD fields, *J. Geophys. Res.*, *102*, 2325.

Birn, J., M. F. Thomsen, J. E. Borovsky, G. D. Reeves, D. J. McComas, R. D. Belian, and M. Hesse (1998), Substorm electron injections: Geosynchronous observations and test particle simulations, *J. Geophys. Res.*, *103*, 9235.

Christon, S. P., D. J. Williams, D. G. Mitchell, L. A. Frank, and C. Y. Huang (1989), Spectral characteristics of plasma sheet ion and electron populations during undisturbed geomagnetic conditions, *J. Geophys. Res.*, *94*, 13,409.

Christon, S. P., D. J. Williams, D. G. Mitchell, C. Y. Huang, and L. A. Frank (1991), Spectral characteristics of plasma sheet ion and electron populations during disturbed geomagnetic conditions, *J. Geophys. Res.*, *96*, 1.

Keiling, A., et al. (2008a), Correlation of substorm injections, auroral modulations, and ground Pi2, *Geophys. Res. Lett.*, *35*, L17S22, doi:10.1029/2008GL033969.

Keiling, A., et al. (2008b), Multiple intensifications inside the auroral bulge and their association with plasma sheet activities, *J. Geophys. Res.*, *113*, A12216, doi:10.1029/2008JA013383.

Kivelson, M. G., S. M. Kaye, and D. J. Southwood (1980), The physics of plasma injection events, in *Dynamics of the Magnetosphere: Proceedings of the AGU Chapman Conference on Magnetospheric Substorms and Related Plasma Processes, Los Alamos, N.M. U.S.A., October 9–13, 1978*, edited by S.-I. Akasofu, p. 385, D. Reidel, Dordrecht, Netherlands.

Kokubun, S., and R. L. McPherron (1981), Substorm signatures at synchronous altitude, *J. Geophys. Res.*, *86*, 11,265.

Konradi, A., C. L. Semar, and T. A. Fritz (1975), Substorm-injected protons and electrons and the injection boundary model, *J. Geophys. Res.*, *80*, 543.

Larson, D., et al. (2009), Solid state telescope for THEMIS, *Space Sci. Rev.*, in press.

Li, X., D. N. Baker, M. Temerin, G. D. Reeves, and R. D. Belian (1998), Simulation of dispersionless injections and drift echoes of energetic electrons associated with substorms, *Geophys. Res. Lett.*, *25*, 3763, doi:10.1029/1998GL900001.

Li, X., T. E. Sarris, D. N. Baker, W. K. Peterson, and H. J. Singer (2003), Simulation of energetic particle injections associated with a substorm on August 27, 2001, *Geophys. Res. Lett.*, *30*(1), 1004, doi:10.1029/2002GL015967.

Liou, K., C.-I. Meng, A. T. Y. Lui, P. T. Newell, and S. Wing (2002), Magnetic dipolarization with substorm expansion onset, *J. Geophys. Res.*, *107*(A7), 1131, doi:10.1029/2001JA000179.

Lopez, R. E., D. G. Sibeck, R. W. McEntire, and S. M. Krimigis (1990), The energetic ion substorm injection boundary, *J. Geophys. Res.*, *95*, 109.

Mauk, B. H., and C. E. McIlwain (1974), Correlation of *Kp* with the substorm-injected plasma boundary, *J. Geophys. Res.*, *79*, 3193.

Mauk, B. H., and C.-I. Meng (1987), Plasma injection during substorms, *Phys. Scr. T*, *18*, 128.

McIlwain, C. E. (1974), Substorm injection boundaries, in *Magnetospheric Physics: Proceedings of the Advanced Summer Institute held at Sheffield, U.K., August 1973*, edited by B. M. McCormac, p. 143, D. Reidel, Dordrecht, Netherlands.

Nagai, T. (1982), Observed magnetic substorm signatures at synchronous altitude, *J. Geophys. Res.*, *87*, 4405.

Raeder, J., D. Larson, W. Li, L. Kepko, and T. Fuller-Rowell (2008), OpenGGCM simulations for the THEMIS mission, *Space Sci. Rev.*, *141*(1–4), 535–555, doi:10.1007/s11214-008-9421-5.

Reeves, G. D., M. G. Henderson, P. S. McLachlan, R. D. Belian, R. H. W. Friedel, and A. Korth (1996), Radial propagation of substorm injections, in *Third International Conference on Substorms*, edited by E. J. Rolfe and B. Kaldeich, *Eur. Space Agency Spec. Publ., ESA SP 389*, p. 579.

Sarris, T., and X. Li (2005), Evolution of the dispersionless injection boundary associated with substorms, *Ann. Geophys.*, *23*, 877.

Sarris, T. E., X. Li, N. Tsaggas, and N. Paschalidis (2002), Modeling energetic particle injections in dynamic pulse fields with varying propagation speeds, *J. Geophys. Res.*, *107*(A3), 1033, doi:10.1029/2001JA900166.

V. Angelopoulos, IGPP, University of California, Los Angeles, CA 90095, USA.

H. U. Auster and K. H. Glassmeier, IGEP, Technical University of Braunschweig, Mendelssohnstrasse 3, D-38106 Braunschweig, Germany.

C. Cully, Swedish Institute of Space Physics, Box 537, SE-751 21 Uppsala, Sweden.

R. Ergun, X. Li, W. L. Liu, and T. Sarris, LASP, University of Colorado, 1234 Innovation Drive, Boulder, CO 80303, USA. (liu@lasp.colorado.edu)

A. Keiling and D. Larson, SSL, University of California, 7 Gauss Way, Berkeley, CA 94720, USA.